HHS Public Access

Author manuscript

Nat Neurosci. Author manuscript; available in PMC 2011 April 01.

Published in final edited form as:

Nat Neurosci. 2010 October ; 13(10): 1233–1239. doi:10.1038/nn.2637.

Clarke's Column Neurons as the Focus of a Corticospinal Corollary Circuit

Adam W. Hantman and **Thomas M. Jessell**

Howard Hughes Medical Institute, Kavli Institute for Brain Science, Depts. of Neuroscience, and Biochemistry and Molecular Biophysics, Columbia University, New York, NY 10032

Thomas M. Jessell: tmj1@columbia.edu

Abstract

Proprioceptive sensory signals inform the CNS of the consequences of motor acts, but effective motor planning involves internal neural systems capable of anticipating actual sensory feedback. Just where and how predictive systems exert their influence remains poorly understood. We have explored the possibility that spinocerebellar neurons that convey proprioceptive sensory information also integrate information from cortical command systems. Analysis of the circuitry and physiology of identified dorsal spinocerebellar tract neurons located in Clarke's column mouse spinal cord reveals distinct populations of Clarke's column neurons that receive direct excitatory and/or indirect inhibitory inputs from descending corticospinal axons. The convergence of these descending inhibitory and excitatory inputs to Clarke's column neurons establishes local spinal circuits with the capacity to mark or modulate incoming proprioceptive input. Together, our genetic, anatomical, and physiological studies provide evidence that Clarke's column spinocerebellar neurons nucleate local spinal corollary circuits of relevance to motor planning and evaluation.

Introduction

The coordination of movement depends on proprioceptive sensory signals which convey the state of muscle activity and body position to motor command centers within the central nervous system1. Proprioceptive afferent input from the limbs is relayed to cortical motor centers along diverse ascending relay pathways, the most prominent of which engages the spinocerebellar system2–4. In mammals, there are a dozen or so distinct classes of spinocerebellar neurons5, each assigned to discrete aspects of somatosensory and motor processing4,6. Proprioceptive sensory signaling from the hindlimb is relayed primarily by a set of dorsal spinocerebellar (dSC) tract neurons that occupy a discrete thoracic and lumbar nucleus called Clarke’s column7,8. Although the sensory relay properties of Clarke’s column have long been appreciated9, the possibility that this set of spinocerebellar neurons

Author contributions

A.W.H. and T.M.J. conceived of the project and planned experiments. A.W.H. performed experiments. A.W.H. and T.M.J. analyzed data and wrote the manuscript.

has additional integrative functions in spinal sensory processing has not been explored in detail.

Proprioceptive sensory information of peripheral origin provides one crucial conduit to the motor system, but there is now emerging evidence that motor systems have the additional capacity to generate internal predictions of the sensory consequences of motor acts10,11. Predictive signals have been argued to provide cortical motor centers with rapid updates about planned actions, helping to obviate delays incurred when proprioceptive feedback is activated from the periphery12,13. Cortically-derived predictions may also be used to negate the sensory consequences of self-generated movements, fine-tuning the motor system to unanticipated sensory events14. Such predictions are thought to be generated by activating corollary pathways which map directly onto sensory processing streams10,11. The cerebellum and cerebral cortex have traditionally been invoked as sites for the convergence of cortical corollary and sensory feedback pathways involved in internal motor predictions15,16, although the local circuitry underlying convergence in these regions is obscure.

The likely existence of distributed sites for supraspinal convergence of motor corollary and sensory feedback pathways prompted us to consider whether corollary convergence might also occur at earlier steps in the proprioceptive processing pathway, perhaps even in the spinal cord. Intriguingly, prior studies of cutaneous sensory coding are consistent with the notion that corollary pathways intersect at early steps of spinal sensory processing17. In addition, physiological studies in the cat by Hongo and coworkers provided evidence that dSC tract neurons can be activated by stimulation of descending cortical tracts18,19. These studies revealed that stimulation of descending corticospinal fibers can result in transient excitation followed by prolonged inhibition of dSC tract neurons18,19, although the particular subclass of spinocerebellar neurons was not determined. The issue of whether and how the output of Clarke's column neurons is shaped by cortical input therefore remains unclear.

To explore the possibility of a spinal focus for convergent cortical corollary and proprioceptive sensory feedback pathways, we have used a combination of molecular genetic, anatomical, and physiological approaches to map the circuitry and integrative functions of identified Clarke's column neurons in the mouse spinal cord. Our anatomical and functional findings reveal that dSC relay neurons in Clarke's column integrate cortical excitatory and inhibitory inputs in a manner capable of mimicking and suppressing proprioceptive feedback. Collectively, these studies provide evidence that Clarke's column neurons nucleate a spinal corollary discharge circuit of potential relevance to motor planning and its evaluation.

Results

dSC neurons marked anatomically and genetically

To map the organization of Clarke's column dSC neurons in mice, we injected fluorogold or cholera toxin B subunit (CTB) into the cerebellum of post-natal day (p) 5–7 animals and monitored the position of retrogradely-labeled neurons at cervical, thoracic, and lumbar

levels of the spinal cord. At caudal thoracic and rostral lumbar levels, retrogradely-labeled neurons were concentrated in the medial region of dorsal horn lamina VII (Fig. 1a), the location of Clarke's column in other mammals20. In the transverse plane, retrogradely-labeled neurons were arrayed in an annular pattern that surrounded a neuron-sparse neuropil core (Fig. 1a, Supplementary Fig. 1). To define the dendritic organization of this set of dSC neurons we injected biocytin into individual fluorogold-labeled neurons. Regardless of their 'clock' position within the annulus, the biocytin-filled dendrites of dSC neurons were oriented towards the core of Clarke's column (Fig. 1e, f).

To provide a way of mapping the trajectory and circuitry of the entire population of Clarke's column neurons, we searched for genetic markers that delineate this subset of spinocerebellar projection neurons. We found that Clarke's column dSC neurons can be defined by selective expression of the *glial derived neurotrophic factor (GDNF)* gene21 (Fig. 1b–d). Endogenous *GDNF* mRNA, as well LacZ expression in a *GDNF*::LacZ transgenic mouse line22, was detected in identified Clarke's column neurons, marked retrogradely by cerebellar fluorogold or CTB injection (Fig. 1a–c). To trace the projections of *GDNF*-expressing dSC neurons, we analyzed GFP expression in mice generated by *GDNF*::CreERT2 transgenic driver and *Tau*::loxP.STOP.loxP. myristoylated (m)GFP (*Tau*::lsl. mGFP)23 reporter crosses. After tamoxifen exposure, the axons of GFP-labeled Clarke's column dSC neurons were detected in the ipsilateral dorsolateral funiculus (Fig. 1g,h) and inferior cerebellar peduncle, and terminated as mossy fibers in the granular layer of the cerebellum (Fig. 1i–m). These GFP-labeled axons were segregated into para-sagittal stripes within cerebellar lobules I, II, III, and VIII (Fig. 1k), consistent with the known organization of dSC projections24. As with biocytin injection, GFP-labeled dendrites of *GDNF*-expressing dSC neurons were confined to the core of Clarke's column (Fig. 1g,h; Supplementary Fig. 1). Thus *GDNF* expression defines Clarke's column dSC neurons, distinguishing them from other dorsal and ventral spinocerebellar projection neurons.

dSC neurons integrate proprioceptive and descending input

We next used anatomical and physiological methods to determine whether Clarke's column dSC neurons receive input from cortical descending as well as proprioceptive sensory pathways.

A *Parvalbumin (Parv)*::GFP bacterial artificial chromosome (BAC) transgenic line25 was used to map the intraspinal projections of proprioceptive axons26. At caudal thoracic and rostral lumbar levels of the spinal cord proprioceptive axonal projections were concentrated in the vicinity of Clarke's column dSC neurons (Fig. 2a). We found that all fluorogold-, CTB- or *GDNF*-labeled dSC neurons were contacted by $Parv^+$ axons labeled in *Parv*::GFP mice, and that that all $Parv^+$ boutons on dSC neurons co-expressed vesicular glutamate transporter-1 (VG1), confirming their sensory synaptic status (Fig. 2b). The vast majority of GFP^+, $VG1^+$ bouton contacts was located on the dendrites of dSC neurons, within the core of Clarke's column (Fig. 2b). In addition, >95% of sensory contacts with Clarke's column dSC neurons, defined by trans-ganglionic transport and accumulation of CTB after hindlimb injection, co-expressed Parv and VG1 (Supplementary Figs. 2–5); an indication27 that almost all direct sensory inputs to dSC neurons derive from proprioceptive afferents.

To determine the functional consequences of proprioceptive input, we recorded from identified dSC neurons in hemisected p8–15 mouse spinal cord preparations (Fig. 3e). Patch-clamp recordings from retrograde fluorogold-labeled dSC neurons at T6 to L2 levels revealed that 56% (47/84) of dSC neurons exhibited excitatory responses to low-threshold stimulation of L4 or L5 dorsal roots (Fig. 3a). Excitatory synaptic potentials recorded from individual dSC neurons exhibited short latencies and low variation in onset time (Fig. 3a, coefficient of variation < 0.05), an indication of their monosynaptic origin. Moreover, dorsal root stimulation elicited action potentials in 84% of responsive dSC neurons (Fig. 3b). Since our anatomical studies revealed that all dSC neurons are contacted by proprioceptive sensory terminals, we presume that the non-responsive dSC population do in fact receive sensory input from afferent axons that enter the spinal cord through other, unstimulated, lumbosacral roots.

To determine whether dSC neurons also receive input from corticospinal axons we first analyzed the spinal cord of *Emx1*::GFP BAC transgenic mice in which axons of cortical origin are marked selectively28. At thoracic and rostral lumbar spinal levels, GFP^+ axons were restricted to the ventral-most aspect of the dorsal funiculus (Fig. 4a) and gave rise to collateral projections that terminated in the vicinity of Clarke's column (Fig. 4a). In *Emx1*::GFP mice, GFP^+ terminals were observed in contact with the cell bodies of about half of all labeled dSC neurons, and many of these GFP^+ terminals expressed PKC-γ, a marker selective for corticospinal axons29 (Fig. 4b; Supplementary Fig. 1). Within the dSC annulus we detected a marked asymmetry in the pattern of corticospinal input: dSC neurons that occupied a dorsomedial position within the annulus received a 12-fold greater density of GFP^+, $VG1^+$ terminal contacts than did dSC neurons in a ventrolateral position, which were contacted by few if any corticospinal axons (Fig. 4a,c; Supplementary Fig. 1). These observations provide anatomical evidence that a subset of Clarke's column dSC neurons in receipt of proprioceptive sensory input are also contacted by the terminals of corticospinal neurons.

To assess the function of these corticospinal inputs we analyzed the response of fluorogold-labeled Clarke's column dSC neurons to focal stimulation of corticospinal axons present in the ventral-most aspect of the dorsal columns, at cervical levels. A series of control anatomical and physiological experiments indicated that dSC neuronal responses to dorsal column stimulation reflect input from corticospinal rather than sensory or spinal neurons (see Supplementary Results and Supplementary Figs. 2–5). Dorsal column stimulation elicited monosynaptic excitatory synaptic responses in ~65% (54/84) of dSC neurons (Fig. 3c). Dorsal column-evoked excitatory input was sufficient to trigger action potentials in ~70% of this set of dSC neurons (Fig. 3d), an indication of the efficacy of corticospinal excitatory drive to these neurons. Moreover, dorsal column-evoked excitatory synaptic responses in dSC neurons were blocked by combined exposure to AMPA and NMDA receptor antagonists (CNQX and AP5 respectively, data not shown), establishing their glutamatergic status.

We also examined directly whether, as implied by the summed incidence of corticospinal and proprioceptive synaptic potentials, individual Clarke's column neurons receive convergent input from these two neuronal classes. Analysis of dSC responses revealed that

synaptic responses to dual dorsal column and dorsal root stimulation were detected in ~55% of sampled dSC neurons, independent of input order or inter-stimulus interval (Fig. 3f). Together, these anatomical and physiological studies indicate that a subset of dSC neurons, presumably those in a dorsomedial annular position, integrate proprioceptive sensory and corticospinal inputs.

Cortically-evoked inhibitory input to dSC neurons

These anatomical and physiological analyses also provided evidence for cortically-evoked inhibitory inputs to Clarke's column neurons. Fluorogold-labeled, and *GDNF*-expressing, dSC neurons were contacted by glutamate decarboxylase 67 $(GAD67)^+$, GABAergic (Fig. 5d,e), and glycine transporter 2 $(GlyT2)^+$, vesicular inhibitory amino acid transporter $(VIAAT)^+$ glycinergic boutons (Fig. 5f). Inhibitory synaptic inputs were detected on dSC neurons at all annular positions. The source of these inhibitory boutons remains unclear, but we did observe a high density of neurons expressing *GAD65, GAD67* (GABAergic) and *GlyT2* (glycinergic) in the regions of the intermediate spinal cord surrounding Clarke's column (Fig. 5a). Furthermore, we found that many peri-dSC GABAergic inhibitory neurons, marked by GFP expression in *GAD65*::GFP transgenic mice30, received dense innervation from $VG1^+$, PKC-γ^+ corticospinal terminals (Fig. 5b,c).

Consistent with these anatomical findings, we found that dorsal column stimulation evoked long-lasting IPSPs in many fluorogold-labeled dSC neurons (Fig. 6a; decay time constant 92 +/− 39 ms; mean +/− standard deviation; n=8 neurons). Overall, 62% of Clarke's column dSC neurons exhibited inhibitory synaptic responses to dorsal column stimulation; with about half of these exhibiting IPSCs alone, and half showing monosynaptic excitatory input prior to inhibition (Fig. 6a,d). IPSPs recorded from dSC neurons were blocked by exposure to both bicuculline and strychnine (Fig. 6b), but were only partially inhibited after application of each antagonist alone, indicating the involvement of both GABAergic and glycinergic inhibitory inputs. In addition, we found that dorsal column stimulation-evoked IPSPs were blocked by the AMPA receptor antagonist CNQX (Fig. 6c), indicating that the inhibitory interneurons that act on dSC neurons are themselves activated by corticospinal input.

The microcircuitry of Clarke's column led us to examine the influence of cortically-activated inhibitory inputs on dSC neuronal responses to sensory stimulation. In the population of dSC neurons that received exclusively inhibitory input, dorsal root-evoked action potentials could be suppressed for ~100 ms following a single conditioning stimulus applied to the dorsal columns (Fig. 7a, 7/7 neurons examined). Similarly, for the set of dSC neurons that exhibited dual excitatory and inhibitory synaptic responses, a single stimulus applied to the dorsal column impaired the ability of sensory stimulation to elicit action potentials (Fig. 7b; 8/8 neurons). Thus, descending corticospinal axons can also suppress dSC neuronal responses to proprioceptive sensory input through the recruitment of local inhibitory interneurons.

Corticospinal and proprioceptive sensory inputs to dSC neurons exhibited an additional inhibitory interaction. In a small subset of dSC neurons that received direct sensory and cortical excitatory inputs in the absence of accompanying IPSPs, dorsal column stimulation

was found to reduce, by ~ 80%, the probability of dorsal root-evoked action potentials (Fig. 7c). This dorsal column-evoked suppression of sensory responses was blocked by exposure to bicuculline and strychnine, despite the lack of detectable IPSPs in these dSC neurons (Fig. 7c). This IPSC-independent inhibitory influence was evident over a period of 50 to 1000 ms, a duration consistently longer than that evoked by post-synaptic inhibition of dSC neurons. One potential substrate for this sustained inhibitory influence is the cortical recruitment of interneurons that exert pre-synaptic inhibitory control of proprioceptive sensory afferent input7,17,31. In support of this possibility, we observed that GFP^+, $VG1^+$ proprioceptive sensory terminals detected on dSC neurons in *Parv*::GFP mice were frequently contacted by GABAergic boutons that co-expressed GAD65 and GAD67 (Fig. 5g) – a cytochemical hallmark of pre-synaptic inhibitory terminals on proprioceptive sensory afferents in the ventral region of mouse spinal cord32. Thus, activation of corticospinal pathways appears to elicit both pre- and post-synaptic inhibition of proprioceptive input to Clarke's column dSC neurons.

Discussion

Our findings show that Clarke’s column dSC neurons represent a focal target for the convergence of descending cortical and sensory afferent pathways, nucleating spinal microcircuits with the potential to predict and modulate proprioceptive feedback signals. Prior physiological studies by Hongo and coworkers have provided evidence for both rapid excitation and prolonged inhibition of dSC neurons by descending corticospinal projections18,19. Our findings are in general agreement with these earlier in vivo studies, although it is worth emphasizing that Hongo’s analysis did not establish the direct nature of cortically-evoked excitation. Nor were Clarke’s column neurons distinguished from other classes of dSC neurons. In fact, the most complete physiological description of dSC neuronal activity and input characteristics was obtained at caudal lumbar segmental levels, a region devoid of Clarke’s column neurons18,19. At these caudal levels, dSC neurons are known to receive prominent direct input from cutaneous sensory afferents6, which contrasts with the nearly pure proprioceptive sensory origin of direct input to Clarke's column neurons. Thus, our findings provide clear evidence for cortical regulation of the activity and output of identified Clarke’s column dSC neurons. When taken together with Hongo’s findings, they suggest a common strategy for descending cortical control of distinct subclasses of dSC neurons.

Our findings also invoke the existence of distinct classes of Clarke’s column dSC neurons. Neurons positioned within the dorsomedial sector of the Clarke’s column annulus can be distinguished from their ventrolateral counterparts by synaptic bouton contacts from corticospinal axons. We presume that these neurons represent the set of physiologically-defined dSC neurons that exhibit excitatory responses to dorsal column stimulation. In addition, dSC neurons throughout the annulus receive dense input from GABAergic and glycinergic inhibitory interneurons, providing a plausible anatomical substrate for the prominent inhibitory responses elicited in most dSC neurons by dorsal column stimulation. Some dSC neurons nevertheless exhibited exclusively excitatory responses to dorsal column stimulation, raising the possibility that the inhibitory boutons that contact some, presumably dorsomedial, dSC neurons derive from interneurons that lack corticospinal input. The

existence of three distinct synaptic arrangements on dSC neurons hints at the operation of multiple channels for proprioceptive processing within Clarke's column (Supplementary Fig. 6a).

Our anatomical analysis of excitatory synaptic terminals on Clarke's column dSC neurons revealed a vast predominance of VG1- over VG2-labeled boutons, and the coexpression of Parv by essentially all $VG1^+$ boutons. This synaptic phenotype implies that virtually all sensory inputs to this set of dSC neurons derive from proprioceptors -- an unanticipated finding when considered from the perspective of physiological studies arguing that dSC neurons serve as sensory monitors of limb position through the convergence of diverse cutaneous and proprioceptive sensory signals. One way of reconciling our findings with prior observations is to invoke the idea that the influence of cutaneous sensory input on the integrative sensory properties of Clarke's column dSC neurons is achieved indirectly, via intermediary interneuronal pathways.

The functional circuitry of dSC neurons uncovered through our physiological analysis of dorsal column inputs provides evidence that Clarke's column serves an integrative role well beyond that of a simple sensory relay nucleus. The existence of strong excitatory cortical inputs to a subset of dSC neurons provides a potential intraspinal pathway for the transfer of descending cortical commands onto a sensory relay system destined for the cerebellum (Supplementary Fig. 6a–i,ii). These cortically-derived signals appear well-suited to deliver predictions of the sensory consequences of motor acts, anticipating peripherally-derived sensory feedback. The cortically-evoked inhibitory responses detected in dSC neurons typically persist for 100msec or more, a period which spans the temporal delay incurred through peripheral routing of proprioceptive sensory feedback33. These findings argue in favor of an independent function for descending cortical commands in suppressing or modulating the impact of activation of dSC neurons by proprioceptive sensory feedback (Supplementary Fig. 6a–iii). The origin of dorsal column inputs to Clarke's column dSC neurons, from motor and/or somatosensory cortical areas, remains to be resolved.

The functions invoked for Clarke's column dSC neurons in the regulation of proprioceptive sensory processing share certain features in common with the integrative properties of ventral spinocerebellar (vSC) tract pathways. Physiological studies have shown that vSC tract neurons receive inputs from sensory, local and descending axons that mirror those converging on spinal motor neurons34,35. One major role of the vSC tract therefore appears to be to relay a corollary copy of inputs to spinal motor neurons directly to supraspinal processing centers36. By analogy, our findings imply that dSC neurons might serve a similar corollary function, with the notable difference that information conveyed via the Clarke's column pathway reports on anticipated proprioceptive input, rather than on imminent motor output. In turn, these considerations pose the downstream problem of how the cerebellum integrates inputs from multiple spinocerebellar signaling streams. In recent genetic tracing studies (AWH and TMJ, data not shown) we have found that the terminals of dSC and vSC axons converge on the same cerebellar folia, and are frequently be found in proximity to the same granule neuron, suggesting that cerebellar processing involves the convergence of spinal inputs onto a common granule cell target.

Intriguingly, the intraspinal circuitry for cortically-mediated inhibition of dSC signaling exhibits an organization that conforms to that of an insect corollary discharge circuit employed in the cancellation of self-generated auditory stimuli37. Mammalian and arthropod circuits both rely on the activation of interneurons that exert pre-synaptic inhibition of sensory afferent input, as well as post-synaptic inhibition of a primary central relay neuron. The additional, predictive, role of dSC neurons uncovered in our studies may be more akin to the corollary activities observed the sensory processing centers of higher mammals12,38. In the mouse, the molecular delineation of dSC neurons opens the way for future genetic manipulation of neuronal elements in this spinal corollary circuit.

Traditionally, corollary discharge circuits involved in motor planning have been assigned to pontocerebellar and intracortical pathways15,16, raising the further question of the merits of constructing intraspinal circuits with similar design features (Supplementary Fig. 6b). A spinally-focused corollary circuit will inevitably incur slightly greater temporal delays than its supraspinal counterparts. But, by way of compensation, it affords descending cortical systems direct access to a selective sensory channel, in principle permitting early and effective anticipation or cancellation of the proprioceptive consequences of movement.

Methods

Retrograde neuronal labeling

Retrograde labeling of spinal cord neurons projecting to the cerebellum was performed as described40 using both fluorogold (Fluorochrome, LLC) and CTB (Vector Laboratories, Inc.) tracers with a minimum of 3 days of transport. Mice (p5–7) were subjected to hypothermic anesthesia, the skin covering the skull was cleaned, 500 nl of retrograde label was delivered to the cerebellum using a PB600 repeating dispenser (Hamilton Co.) with a 26 gauge needle, the needle was slowly retracted, the surface of the head recleaned, the animal warmed and returned to its cage. The needle was manually guided into the cerebellum and the injection site was evaluated by examining residual tracer at the injection site and by the pattern of retrograde labeling.

In situ hybridization histochemistry

Probes for *in situ* hybridization detection of *GDNF*, *GAD65*, *GAD67* and *GlyT2* mRNA were generated using PCR and TOPO cloning (Invitrogen Co). *In situ* hybridization histochemistry was performed on cryostat sections (20 μm). For dual label *in situ* hybridization histochemistry and retrograde labeling, spinal cord sections were cut, each section registered, fluorogold-labeling photographed at two different magnifications, sections hybridized with *GDNF* probe, resulting hybridization signal photographed, and images of fluorogold and hybridization label superimposed.

LacZ staining

LacZ activity was visualized using a standard X-Gal staining protocol. *GDNF*::LacZ mice were perfused with 4% paraformaldehyde and post-fixed for a maximum of 3h. Spinal cord tissue was hemisected or transversely sectioned (100 μm) with a vibratome.

Biocytin-labeling and electrophysiology

Biocytin-labeling and electrophysiology were performed as described41. Fluorogold was injected 3 or more days prior to biocytin-labeling and electrophysiology. Animals were decapitated, the vertebral column removed, and a laminectomy performed. After removal of the dura, lumbar dorsal roots were cut proximal to the dorsal root ganglia, and the spinal cord was cut along the ventral midline to the dorsal columns. The spinal cord was removed from the vertebral column, incubated in artificial cerebrospinal fluid [(in mM): 125 NaCl, 26 $NaHCO_3$, 1.25 NaH_2PO_4, 2.5 KCl, 2 $CaCl_2$, 1 $MgCl_2$, 0.4 ascorbic acid, 2 pyruvate, and 26 D-glucose, and equilibrated with 95% O_2 and 5% CO_2] for 1 hr, and then positioned in a chamber (Warner Instruments, LLC). A lumbar dorsal root (L4 to L6) was drawn into a suction electrode and a concentric bipolar electrode (FHC, Inc.) was positioned with a micromanipulator (MP-285, Sutter Instruments Co.) on the ventral aspect of the dorsal column in cervical spinal cord. To selectively stimulate cortical axons, the corticospinal tract was mapped using GFP fluorescence in hemisected preparations from *Emx-1*::GFP transgenic mice. This position was identified in non-GFP expressing tissue using infrared-differential interference contrast (IR-DIC) imaging.

Electrophysiological experiments were performed on hemisected spinal cord preparations of p10–15 mice, at room temperature. Fluorogold-labeled dSC neurons, revealed by fluorescence and IR-DIC imaging, were selected from T6–L2 spinal levels. This ensured a minimum six segment separation between the dorsal column stimulation electrode and the recording site. Whole-cell, patch-clamp recordings (internal pipette contents in mM: 130 potassium gluconate, 5 NaCl, 1 $CaCl_2$, 1 $MgCl_2$, 10 HEPES, and 4 Na_2ATP) were obtained from fluorogold-labeled dSC neurons with resting membrane potentials < −50 mV. Evoked responses were assayed (MultiClamp 700B; MDS, Inc.) from graded stimulation (S88 Grass stimulator; Astro-med, Inc.) through the suction electrode (dorsal roots, sensory axons) or the concentric bipolar electrode (dorsal column, corticospinal tract). Pharmacological experiments were performed by adding drugs (Sigma Aldrich Co.) to the superfusate. For biocytin-labeling, spinal tissue containing biocytin-filled neurons were fixed for a minimum of 12h and processed for immunohistochemistry.

Tamoxifen injection

To induce Cre recombination and mGFP expression in dSC neurons, tamoxifen (0.5 to 1mg, Sigma Aldrich Co.) was injected intraperitoneally in ~ 5g, p5–7 mice and the tissue harvested 3–7 days after injection. Tamoxifen ([10 mg/ml], Sigma Aldrich Co.) was dissolved in sesame oil (Sigma Aldrich Co.) and ethanol, at 37°C.

Immunohistochemistry

Immunohistochemistry was performed on cryostat and vibratome sections through sequential exposure to primary antibodies and fluorophore-conjugated secondary antibodies (Jackson Immunoresearch, Inc). Vibratome sections (80–250 μm) were incubated in primary antibodies for 3 days at 4° C and secondary antibodies for 1 day at 4° C.

Confocal microscopy

Confocal images were taken with a LSM 710 microscope (Carl Zeiss, Inc.) with a motorized stage to facilitate the creation of montage images. Configurations for high-magnification images were set for thick vibratome sections of cerebellum. Stage x-y coordinates covering the entire specimen were determined and the Zeiss Multi-time macro was used to assemble montage high-resolution images.

Mice

We used p10–p21 *Parv*::GFP and *Emx1*::GFP mice to map proprioceptive (*Parv*) and cortical (*Emx1*) inputs to retrogradely- or genetically-labeled dSC neurons. Mice used in this study: *GDNF*::LacZ mice22, *GDNF*::CreERT2 a generous gift from Frank Costantini (to be described in a later publication), *GAD65*::GFP30, *Parv*::GFP25, *Emx1*::GFP (MMRRC-GENSAT), *Emx1*::Cre39, *Parv*::Cre and *Tau*::lsl. mGFP23. Procedures performed in this study were approved by the Institutional Animal Care and Use Committee of Columbia University.

Antibodies

Antibodies used: goat and chick anti-LacZ from Biogenesis Ltd and Abcam, Inc.; rabbit and chick anti-GFP from Invitrogen Co. and Aves Lab, Inc.; rabbit and guinea pig anti-VG1 from Synaptic Systems GmH and 32; mouse and rabbit anti-GAD67 from Chemicon, Inc. and 32; guinea pig anti-GlyT2 from Chemicon, Inc., rabbit anti-VGAT from 32, and rat and mouse anti-GAD65 from 32.

Supplementary Material

Refer to Web version on PubMed Central for supplementary material.

Acknowledgments

We thank B. Han and K. Miao for technical assistance; J. de Nooij and G. Sürmeli for help in retrograde labeling of proprioceptive afferents; J. Kirkland and M. Mendelsohn for animal care; and K. MacArthur and I. Schieren for help in preparing the manuscript. We are grateful to S. Arber, N. Asai, C Cebrian, Z.J. Huang, J. Milbrandt, J. Sanes, G. Szabo, and MMRCC-GENSAT for mouse lines, and especially to F. Costantini for permission to use unpublished *GDNF*::CreERT2 mice. We thank R. Axel, M. Churchland, K. Franks, S. Grillner, J. Krakauer, C. Miall, S. Poliak, K. Ritola, D. Stettler, and D. Wolpert for discussion and/or comments on the manuscript. A.W. Hantman was supported by the Howard Hughes Medical Institute and the Robert Leet and Clara Guthrie Patterson Trust Fellowship. T.M. Jessell was supported by grants from the NINDS, The Wellcome Trust, the G Harold and Leila Y Mathers Foundation, Project A.L.S and is an Investigator of the Howard Hughes Medical Institute.

References

1. Eccles JC, Oscarsson O, Willis WD. Synaptic action of group I and II afferent fibres of muscle on the cells of the dorsal spinocerebellar tract. J Physiol. 1961; 158:517–543. [PubMed: 13889058]
2. Lundberg A. Ascending Spinal Hindlimb Pathways in the Cat. Prog Brain Res. 1964; 12:135–163. [PubMed: 14202436]
3. Oscarsson O. Functional Organization of the Spino- and Cuneocerebellar Tracts. Physiol Rev. 1965; 45:495–522. [PubMed: 14337566]
4. Bosco G, Poppele RE. Proprioception from a spinocerebellar perspective. Physiol Rev. 2001; 81:539–568. [PubMed: 11274339]

5. Matsushita M, Hosoya Y. Cells of origin of the spinocerebellar tract in the rat, studied with the method of retrograde transport of horseradish peroxidase. Brain Res. 1979; 173:185–200. [PubMed: 90539]
6. Edgley SA, Jankowska E. Information processed by dorsal horn spinocerebellar tract neurones in the cat. J Physiol. 1988; 397:81–97. [PubMed: 3411521]
7. Walmsley B. Central synaptic transmission: studies at the connection between primary afferent fibres and dorsal spinocerebellar tract (DSCT) neurones in Clarke's column of the spinal cord. Prog Neurobiol. 1991; 36:391–423. [PubMed: 1653444]
8. Hongo T, et al. Trajectory of group Ia and Ib fibers from the hind-limb muscles at the L3 and L4 segments of the spinal cord of the cat. J Comp Neurol. 1987; 262:159–194. [PubMed: 3624550]
9. Mann MD. Clarke's column and the dorsal spinocerebellar tract: a review. Brain Behav Evol. 1973; 7:34–83. [PubMed: 4349416]
10. Wolpert DM, Ghahramani Z, Jordan MI. An internal model for sensorimotor integration. Science. 1995; 269:1880–1882. [PubMed: 7569931]
11. Wolpert DM, Miall RC. Forward models for physiological motor control. Neural Netw. 1996; 9:1265–1279. [PubMed: 12662535]
12. Sommer MA, Wurtz RH. A pathway in primate brain for internal monitoring of movements. Science. 2002; 296:1480–1482. [PubMed: 12029137]
13. Jeannerod, M. Motor cognition : what actions tell the self. Oxford University Press; 2006. p. 1-21.
14. Roy JE, Cullen KE. Selective processing of vestibular reafference during self-generated head motion. J Neurosci. 2001; 21:2131–2142. [PubMed: 11245697]
15. Mulliken GH, Musallam S, Andersen RA. Forward estimation of movement state in posterior parietal cortex. Proc Natl Acad Sci U S A. 2008; 105:8170–8177. [PubMed: 18499800]
16. Ebner TJ, Pasalar S. Cerebellum predicts the future motor state. Cerebellum. 2008; 7:583–588. [PubMed: 18850258]
17. Seki K, Perlmutter SI, Fetz EE. Sensory input to primate spinal cord is presynaptically inhibited during voluntary movement. Nat Neurosci. 2003; 6:1309–1316. [PubMed: 14625555]
18. Hongo T, Okada Y. Cortically evoked pre- and postsynaptic inhibition of impulse transmission to the dorsal spinocerebellar tract. Exp Brain Res. 1967; 3:163–177. [PubMed: 6031545]
19. Hongo T, Okada Y, Sato M. Corticofugal influences on transmission to the dorsal spinocerebellar tract from hindlimb primary afferents. Exp Brain Res. 1967; 3:135–149. [PubMed: 6031544]
20. Mott F. Microscopical examination of Clarke's Column in man, the monkey, and the dog. J Anat Physiol. 1888; 22:479–495.
21. Nosrat CA, et al. Cellular expression of GDNF mRNA suggests multiple functions inside and outside the nervous system. Cell Tissue Res. 1996; 286:191–207. [PubMed: 8854888]
22. Moore MW, et al. Renal and neuronal abnormalities in mice lacking GDNF. Nature. 1996; 382:76–79. [PubMed: 8657308]
23. Hippenmeyer S, et al. A developmental switch in the response of DRG neurons to ETS transcription factor signaling. PLoS Biol. 2005; 3:e159. [PubMed: 15836427]
24. Matsushita M, Gao X. Projections from the thoracic cord to the cerebellar nuclei in the rat, studied by anterograde axonal tracing. J Comp Neurol. 1997; 386:409–421. [PubMed: 9303426]
25. Dumitriu D, Cossart R, Huang J, Yuste R. Correlation between axonal morphologies and synaptic input kinetics of interneurons from mouse visual cortex. Cereb Cortex. 2007; 17:81–91. [PubMed: 16467567]
26. Yoshida Y, Han B, Mendelsohn M, Jessell TM. PlexinA1 signaling directs the segregation of proprioceptive sensory axons in the developing spinal cord. Neuron. 2006; 52:775–788. [PubMed: 17145500]
27. Alvarez FJ, Villalba RM, Zerda R, Schneider SP. Vesicular glutamate transporters in the spinal cord, with special reference to sensory primary afferent synapses. J Comp Neurol. 2004; 472:257–280. [PubMed: 15065123]
28. Bareyre FM, Kerschensteiner M, Misgeld T, Sanes JR. Transgenic labeling of the corticospinal tract for monitoring axonal responses to spinal cord injury. Nat Med. 2005; 11:1355–1360. [PubMed: 16286922]

29. Finger JH, et al. The netrin 1 receptors Unc5h3 and Dcc are necessary at multiple choice points for the guidance of corticospinal tract axons. J Neurosci. 2002; 22:10346–10356. [PubMed: 12451134]
30. Lopez-Bendito G, et al. Preferential origin and layer destination of GAD65-GFP cortical interneurons. Cereb Cortex. 2004; 14:1122–1133. [PubMed: 15115742]
31. Lomeli J, Quevedo J, Linares P, Rudomin P. Local control of information flow in segmental and ascending collaterals of single afferents. Nature. 1998; 395:600–604. [PubMed: 9783585]
32. Betley JN, et al. Stringent specificity in the construction of a GABAergic presynaptic inhibitory circuit. Cell. 2009; 139:161–174. [PubMed: 19804761]
33. Prochazka A, Gillard D, Bennett DJ. Implications of positive feedback in the control of movement. J Neurophysiol. 1997; 77:3237–3251. [PubMed: 9212271]
34. Arshavsky YI, Berkinblit MB, Fukson OI, Gelfand IM, Orlovsky GN. Origin of modulation in neurones of the ventral spinocerebellar tract during locomotion. Brain Res. 1972; 43:276–279. [PubMed: 5050196]
35. Arshavsky Yu I, Gelfand IM, Orlovsky GN, Pavlova GA, Popova LB. Origin of signals conveyed by the ventral spino-cerebellar tract and spino-reticulo-cerebellar pathway. Exp Brain Res. 1984; 54:426–431. [PubMed: 6723862]
36. Lundberg A. Function of the ventral spinocerebellar tract. A new hypothesis. Exp Brain Res. 1971; 12:317–330. [PubMed: 5553376]
37. Poulet JF, Hedwig B. The cellular basis of a corollary discharge. Science. 2006; 311:518–522. [PubMed: 16439660]
38. Blakemore SJ, Sirigu A. Action prediction in the cerebellum and in the parietal lobe. Exp Brain Res. 2003; 153:239–245. [PubMed: 12955381]
39. Gorski JA, et al. Cortical excitatory neurons and glia, but not GABAergic neurons, are produced in the Emx1-expressing lineage. J Neurosci. 2002; 22:6309–6314. [PubMed: 12151506]
40. Arsenio Nunes ML, Sotelo C. Development of the spinocerebellar system in the postnatal rat. J Comp Neurol. 1985; 237:291–306. [PubMed: 3840179]
41. Hantman AW, van den Pol AN, Perl ER. Morphological and physiological features of a set of spinal substantia gelatinosa neurons defined by green fluorescent protein expression. J Neurosci. 2004; 24:836–842. [PubMed: 14749428]

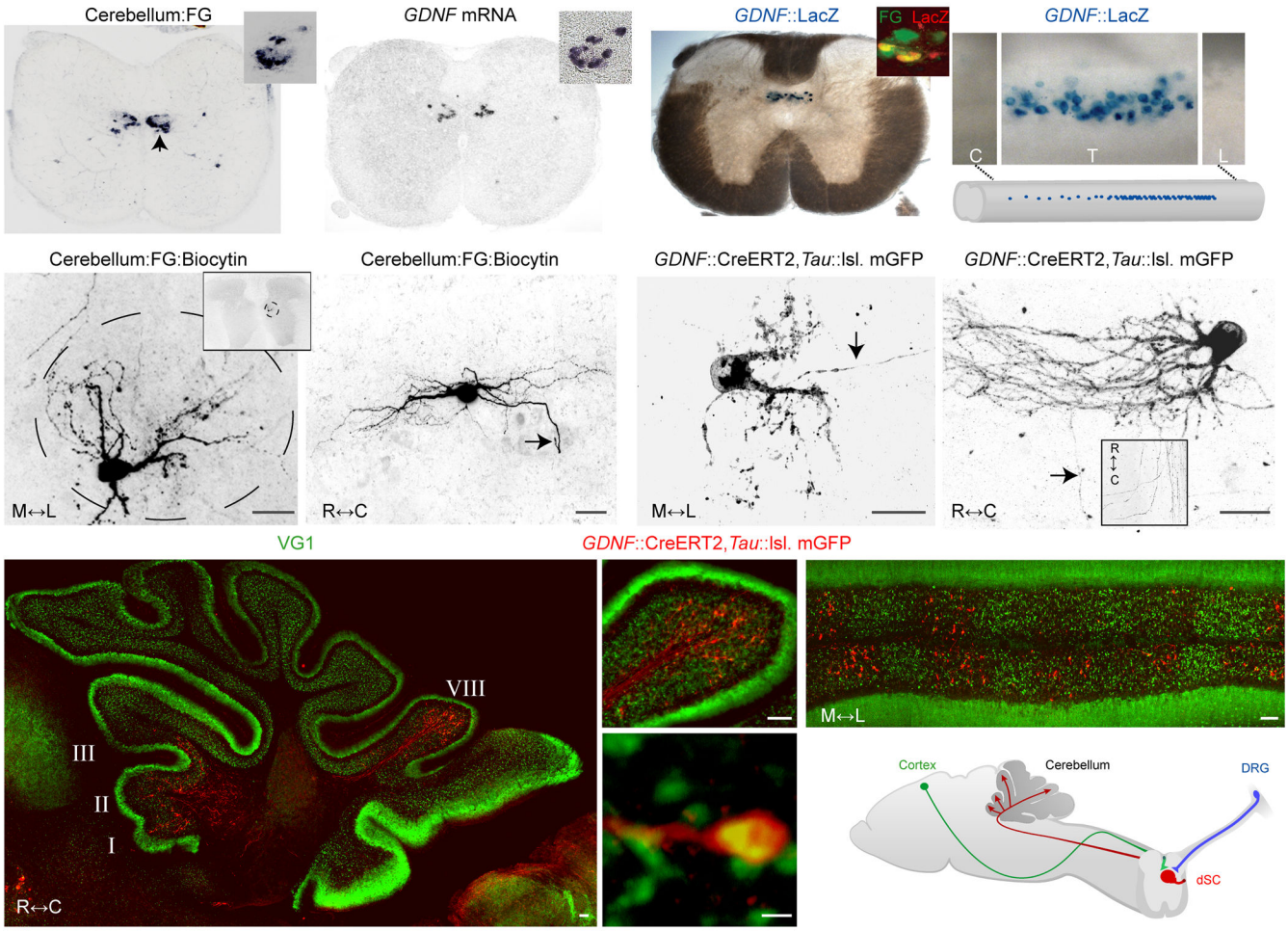

Figure 1. Anatomic and genetic characterization of post-natal mouse dSC neurons

(a) Location of thoracic spinal neurons retrogradely-labeled from cerebellum with fluorogold (FG). Clarke's column marked by arrowhead; inset, high-magnification of FG in Clarke's column. **(b)** *GDNF* mRNA expression in thoracic spinal cord (inset, *GDNF* expression in Clarke's column of **a** inset). A small group of retrogradely-labeled, *GDNF*-expressing neurons are also found in the deep dorsal horn. **(c)** LacZ activity in *GDNF*::LacZ spinal cord (inset, co-labeling of LacZ and retrograde fluorogold label from the cerebellum in Clarke's column). **(d)** Upper, *GDNF* neurons along the rostral-caudal axis (C, cervical; T, thoracic; L, caudal lumbar). Lower, summary of dSC distribution. High density in caudal thoracic levels; low density in rostral thoracic; and absent in cervical, caudal lumbar, and sacral (not shown) levels. **(e)** Morphology of a biocytin-filled, fluorogold$^+$ dSC neuron in a transverse section (inset, low-magnification image; scale bar, 25μm) and **(f)** in a sagittal section (arrow marks axon; scale bar, 50μm). **(g)**, Morphology of *GDNF*::CreERT2, *Tau*::lsl. mGFP$^+$ dSC neurons (arrow marks axon) in a transverse section and **(h)** in a sagittal section (arrow marks axon; inset, horizontal spinal section of dorsal lateral funiculus). Scale bars **g,h**; 25μm. **i**, *GDNF*::CreERT2, *Tau*::lsl. mGFP$^+$ dSC axons in a sagittal section of cerebellum. **(j)** Magnified image of *GDNF*::CreERT2, *Tau*::lsl. mGFP$^+$ dSC axons of lobule VIII of **i**. **(k)** *GDNF*::CreERT2, *Tau*::lsl. mGFP$^+$ dSC axons in a

coronal section of cerebellum. Scale bars **i–k**, 50μm. **(l)** VG1 expression in *GDNF*::CreERT2, *Tau*::lsl. $mGFP^{+}$ dSC axons. Scale bar, 1μm. **(m)** Summary of dSC anatomy (DRG, dorsal root ganglia).

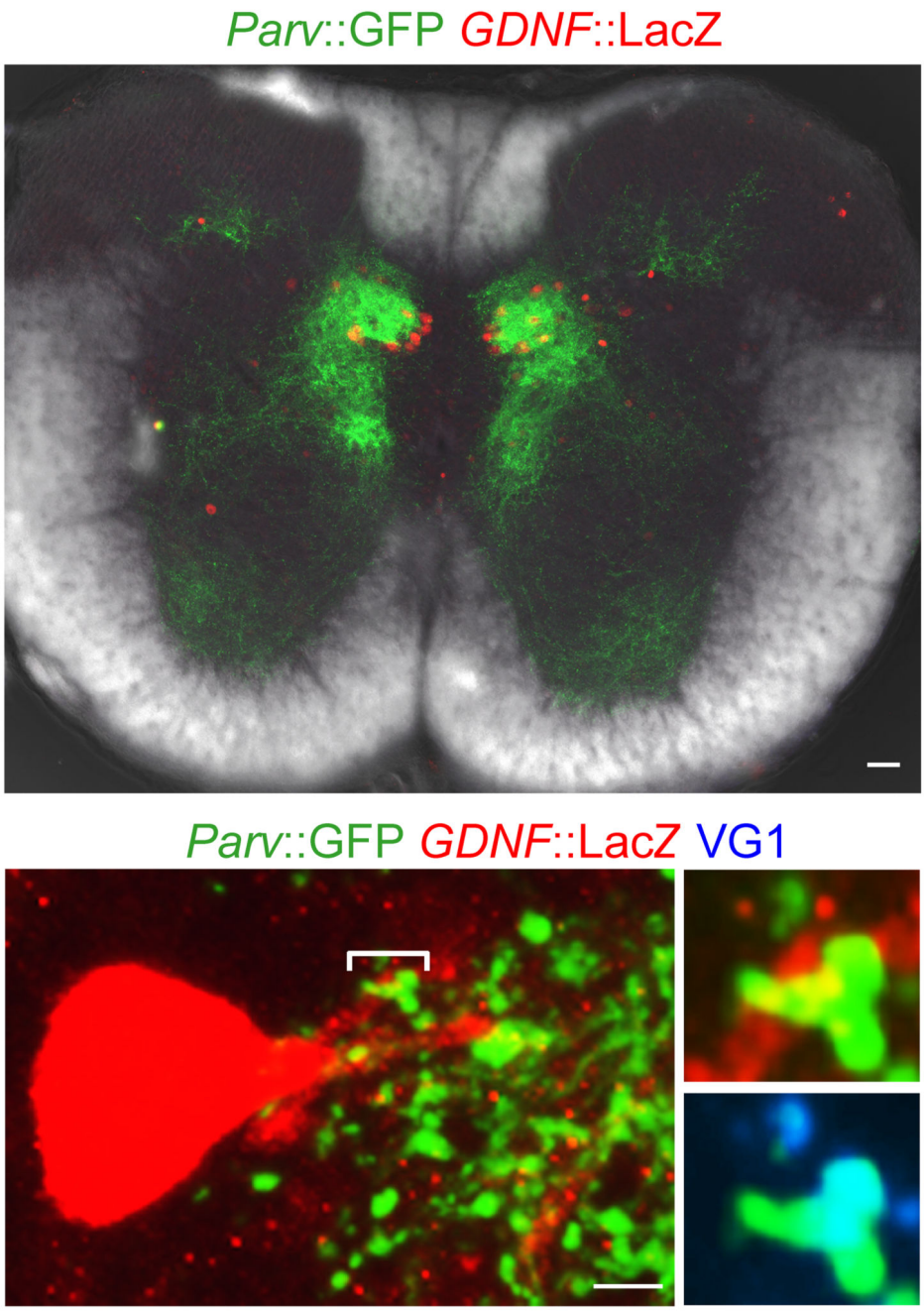

Figure 2. Anatomy of proprioceptive inputs to dSC neurons

(a) Low-magnification image of thoracic spinal cord including *Parv*::GFP^{+} expressing proprioceptor terminals and *GDNF*::LacZ^{+} dSC neurons. Scale bar, 50μm. **(b)** *Parv*::GFP^{+} expressing proprioceptor terminals on an individual *GDNF*::LacZ^{+} dSC neuron (right-top, high-magnification image of bracketed area; right-bottom, *Parv* and VG1 expression of bracketed area). Scale bar, 5μm.

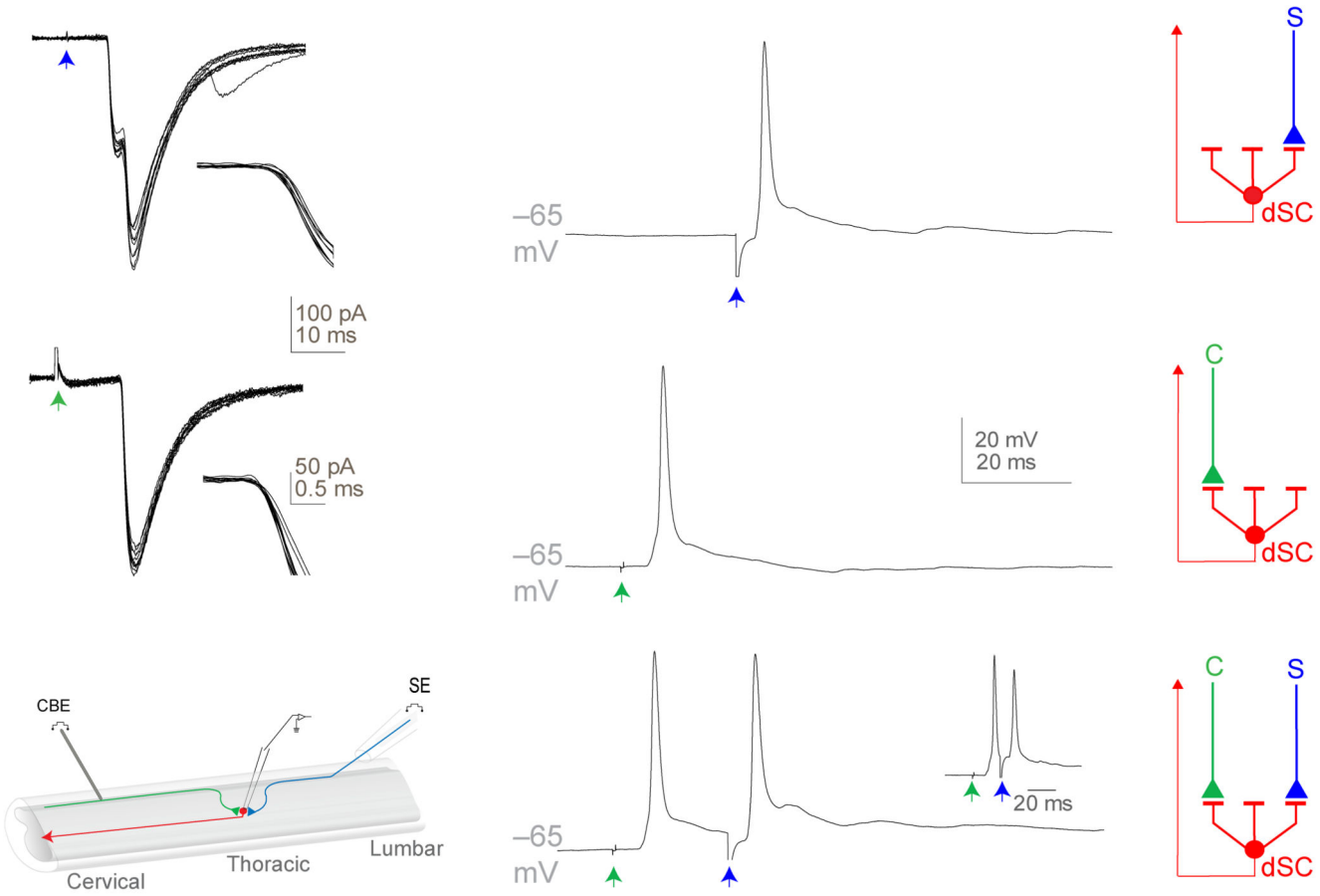

Figure 3. Physiology of proprioceptive and cortical inputs to dSC neurons

(a) 10 dorsal root (blue arrow)-evoked EPSCs in a dSC neuron (inset, expanded time scale around response onset). **(b)** Single dorsal root-evoked EPSP in a dSC neuron, dorsal root-evoked action potentials were detected in 26/31 neurons. Schematic of sensory (S, blue) input to dSC neurons. **(c)** 10 dorsal column (green arrow)-evoked EPSCs in a dSC neuron (inset, expanded time scale around response onset). **(d)** Single dorsal column-evoked EPSP in a dSC neuron, dorsal column-evoked action potentials were generated in 14/20 neurons. Schematic of cortical (C, green) input to dSC neurons. **(e)** Hemisected spinal cord preparation. Lumbar (L4–L6) dorsal roots (blue) were stimulated with a suction electrode (SE) and cervical dorsal column (green) was stimulated with a concentric bipolar electrode (CBE). **(f)** EPSPs of dSC neurons recorded after dorsal root and dorsal column stimulation (inset, reduced interstimulus interval between dorsal root and dorsal column stimulation). Schematic of convergence of cortical and sensory inputs on dSC neurons.

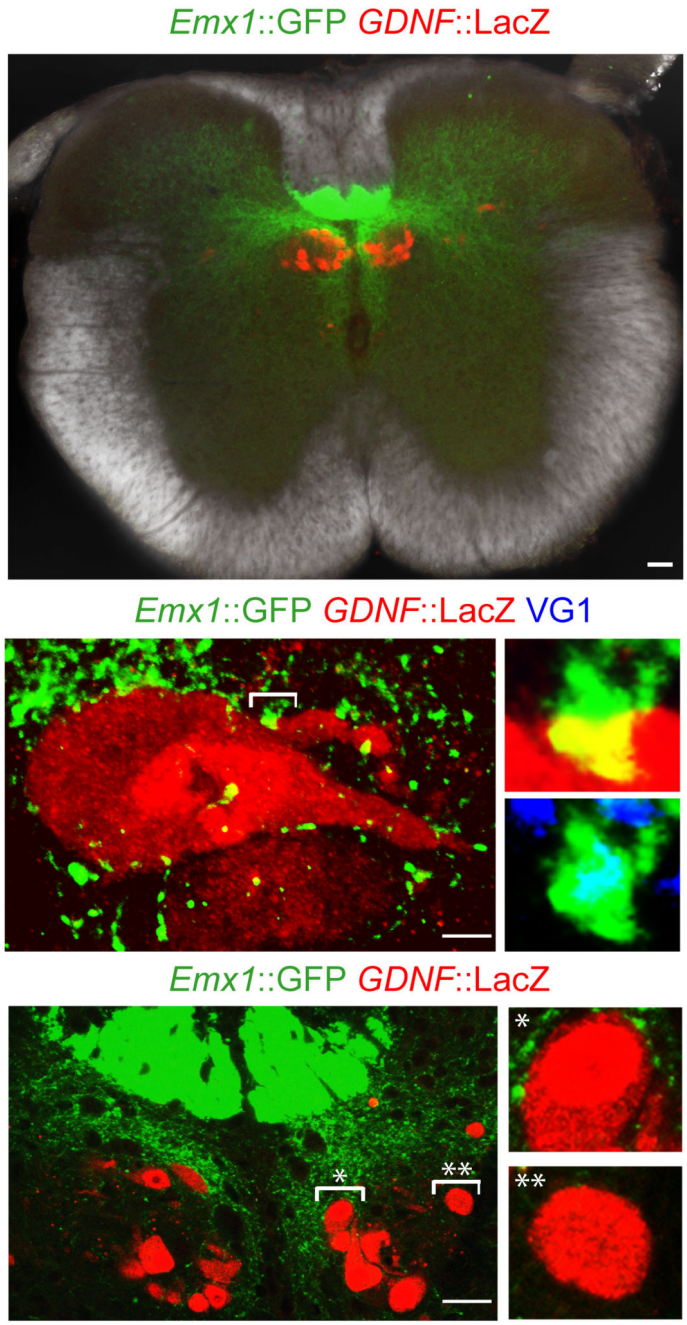

Figure 4. Anatomy of cortical inputs to dSC neurons

(a) Low-magnification image of thoracic spinal cord including *Emx1*::GFP$^+$ expressing corticospinal terminals and *GDNF*::LacZ$^+$ dSC neurons. Scale bar, 50μm. **(b)** *Emx1*::GFP$^+$ corticospinal terminals on an individual *GDNF*::LacZ$^+$ dSC neuron (right-top, high-magnification image of bracketed area; right-bottom, GFP and VG1 expression of bracketed area). Scale bar, 5μm. **(c)** Organization of *Emx1*::GFP$^+$ corticospinal terminals with respect to location of *GDNF*::LacZ$^+$ dSC neurons (right-top, magnified image of * bracketed area; right-bottom, magnified image of ** bracketed area). Scale bar, 25μm.

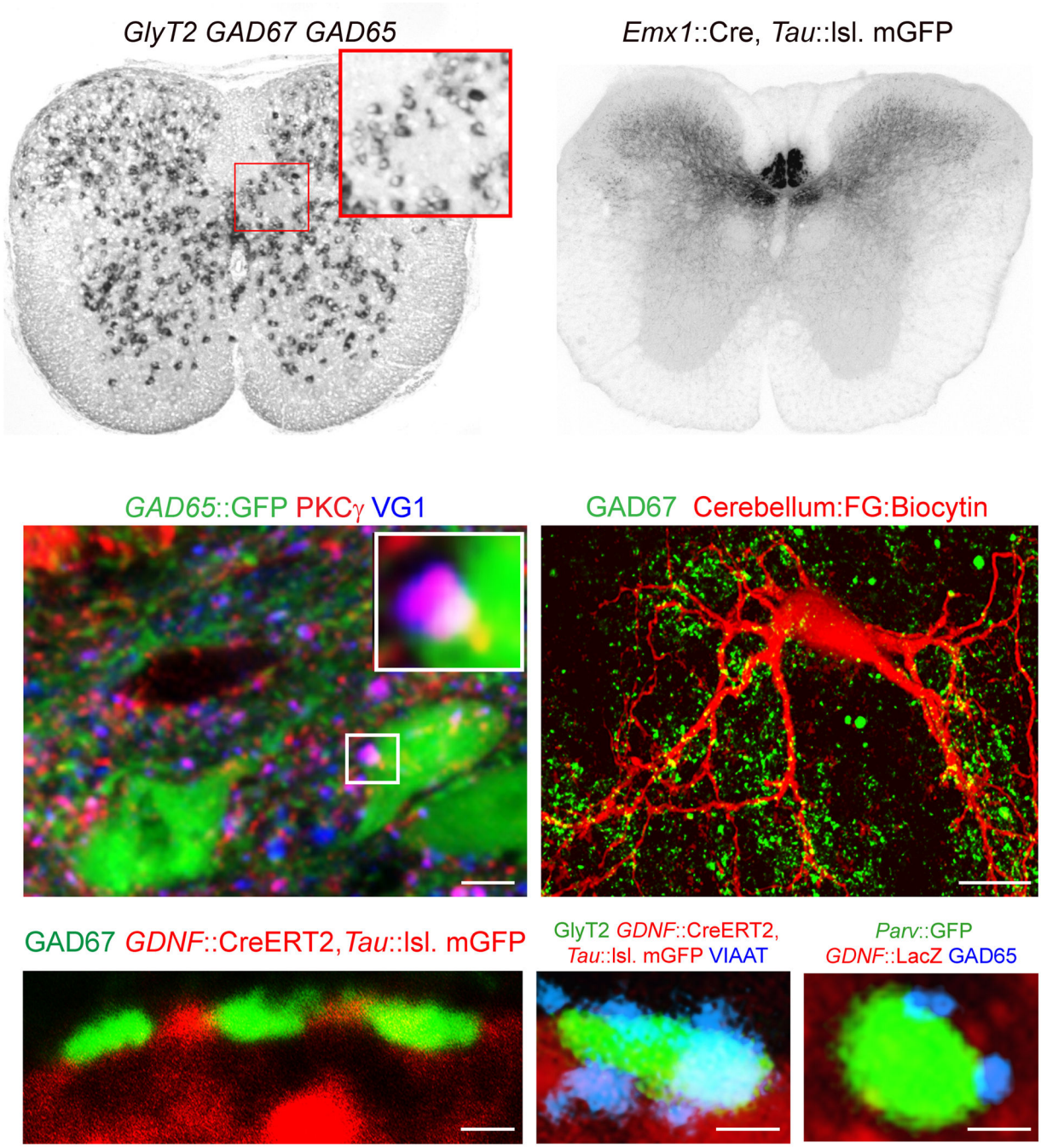

Figure 5. Anatomy of cortically-evoked inhibition of dSC neurons

(a) *In situ* hybridization of *GlyT2*, *GAD67*, and *GAD65* probes in thoracic spinal cord (inset, magnified image of boxed area). **(b)** Distribution of *Emx1*::Cre, *Tau*::lsl. mGFP^{+} corticospinal terminals39 in thoracic spinal cord. **(c)** Apposition of PKC-γ^{+}, VG1^{+} corticospinal terminals and *GAD65*::GFP^{+} neurons (inset, magnified image of boxed area). Scale bar, 5μm. **(d)** GAD67^{+} inhibitory inputs on a biocytin-filled dSC neuron. Scale bar, 50μm. **(c)** GABAergic (GAD67^{+}) and **(f)** glycinergic (GlyT2^{+} and VIAAT^{+}) inhibitory

inputs on *GDNF*::CreERT2, *Tau*::lsl. mGFP^{+} dSC neurons. **(g)** GAD65^{+} inhibitory terminals on *Parv*::GFP^{+} proprioceptive terminals in Clarke's column. Scale bars **e–g**, 1μm.

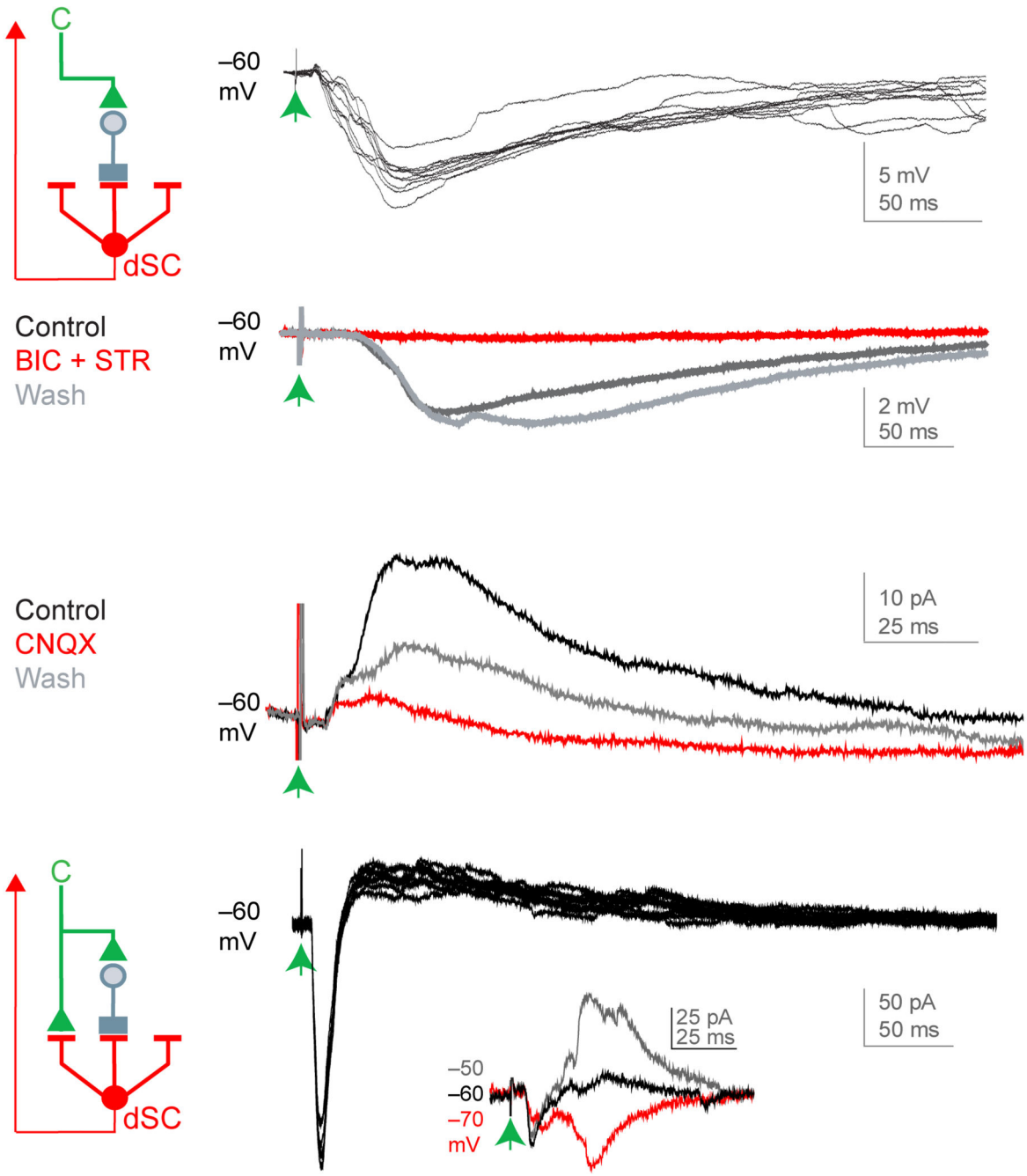

Figure 6. Physiology of cortically-evoked inhibition of dSC neurons

(a) Left, schematic of cortical excitation (green) of an inhibitory input (gray) to dSC neurons. Right, 10 dorsal column-evoked IPSPs in a dSC neuron. **(b)** Pharmacological assessment of bicuculline (BIC, $GABA_A$-receptor antagonist, 8 μM) and strychnine (STR, glycine-receptor antagonist, 10 μM) action on dorsal column-evoked IPSPs in a dSC neuron (each trace is average of 10 trials). **(c)** Pharmacological assessment of CNQX (AMPA-receptor antagonist, 10 μM) action on dorsal column-evoked IPSCs of a dSC neuron (each trace is average of 10 trials). **(d)** Left, schematic of cortical excitation (green) and inhibition

(gray) of a dSC neuron. Right, 10 dorsal column-evoked EPSCs and IPSCs in a dSC neuron (inset, reversal potential of inhibitory component).

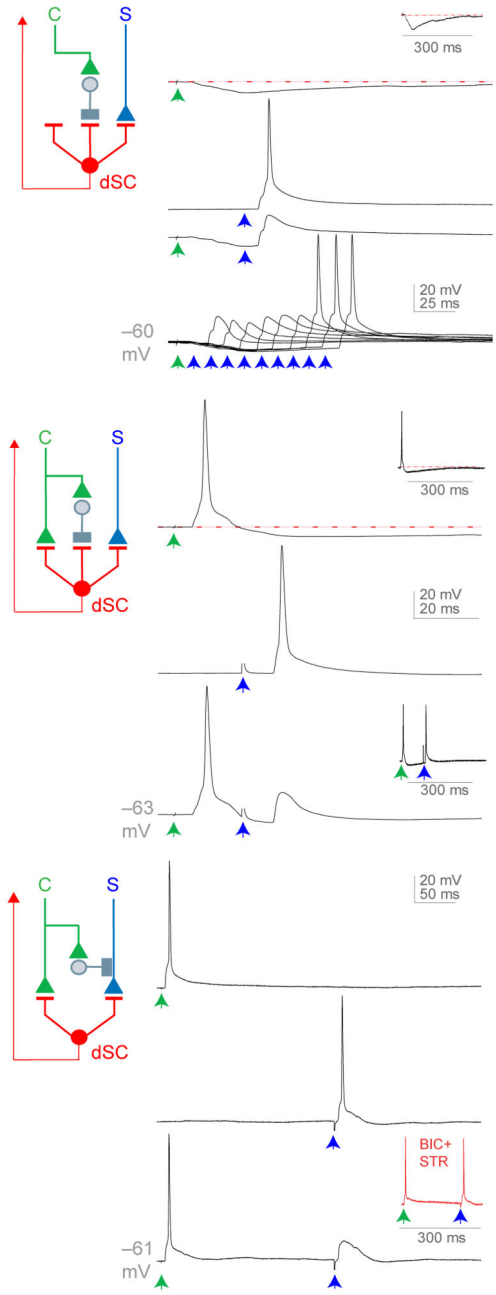

Figure 7. Cortical inhibition of sensory-evoked responses in dSC neurons

Three modes of dorsal column inhibition of dorsal root responses in dSC neurons. **(a)** Top, dorsal column-evoked IPSP in a dSC neuron (inset, longer time scale to show duration of inhibition); second, dorsal root-evoked EPSPs in a dSC neuron; third, dorsal root-evoked EPSP preceded by dorsal column-evoked IPSP; bottom, dorsal root input preceded by dorsal column input at different time intervals. **(b)** Top, dorsal column-evoked EPSP and IPSP in a dSC neuron (inset, longer time scale to show duration of inhibition); middle, dorsal root-evoked EPSP in a dSC neuron; bottom, dorsal root-evoked EPSP preceded by dorsal

column-evoked EPSP and IPSP (inset, longer inter-stimulus interval between dorsal root and dorsal column stimulation). **(c)** Top, dorsal column-evoked EPSP in a dSC neuron; middle, dorsal root-evoked EPSP in a dSC neuron; bottom, dorsal root-evoked EPSP preceded by dorsal column-evoked EPSP (inset, dorsal root input preceded by dorsal column input in the presence of BIC and STR). All traces represent single trials. No IPSPs were detected in this cell, even at depolarized holding potentials. These findings are suggestive of a presynaptic inhibitory mechanism, which could also occur in neurons exhibiting cortically- evoked postsynaptic inhibition.